JOC The Journal of Organic Chemistry

pubs.acs.org/joc Note

Rotational Isomerism of an Amide Substituted Squaraine Dye: A Combined Spectroscopic and Computational Study

Andreas T. Rösch, Serge H. M. Söntjens, Jorn Robben, Anja R. A. Palmans, and Tobias Schnitzer*

Cite This: J. Org. Chem. 2021, 86, 13100−13103 Read Online

ACCESS | Metrics & More | Article Recommendations | Supporting Information

ABSTRACT: The conformational analysis of a 2,4-bis(4-dialkylamino-2-amido)phenyl squaraine dye revealed the presence of two rotational isomers at room temperature. Combination of spectroscopic and computational techniques showed that the rotational barrier is influenced by hydrogen bonds between the amido substituents and the oxygen atoms at the quadratic core. Even small amounts of trifluoroacetic acid interfered with the intramolecular hydrogen bond formation and accelerated the interconversion of the conformers.

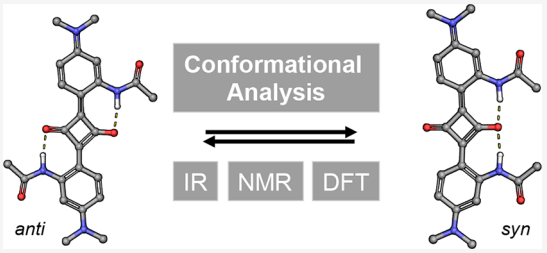

Squaraine dyes attract increasing attention owing to their optoelectronic applications in (bio)labeling,[1−3] photodynamic therapy,[4] organic photodiodes,[5,6] and dye-sensitized[7−10] and organic bulk heterojunction solar cells.[11,12] The broad applicability of the dyes is due to their high absorbance of visible light.[13,14] This absorbance stems from the intramolecular charge transfer between the electron-poor quadratic core and the electron-rich aryl groups.[14] Thus, the optical properties of squaraine dyes can be tuned via the substituents on the aryl groups.

Recently, our group has reported on the aggregation behavior of chiral and achiral amide substituted squaraine dyes and their application in organic spintronics.[15] These dyes contain amide substituents in the *ortho* position of the aryl group to modulate the optoelectronic properties. Yet, *ortho* substituents may restrict the rotation about the aryl−squaraine bond,[16−21] which potentially influences the material properties of squaraine dyes. The group of Kazmaier et al.[17] reported on rotational isomers of a squaraine derivative with 2-hydroxyphenyl groups capable of forming intramolecular hydrogen bonds.[17] We envisioned that the 2-amidophenyl groups in our dyes are also capable of intramolecular hydrogen bonds, thereby leading to a hindered rotation (Scheme 1).

Scheme 1. Proposed Conformers of 1, R = *n*-Heptyl

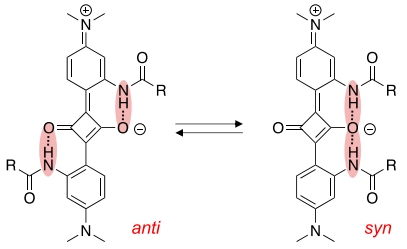

Herein, we study the rotational isomerization of squaraine dye **1** bearing 2-amidophenyl substituents (Scheme 1). Using combined Fourier transform-infrared (FT-IR), ^{1}H and ^{13}C{1H} nuclear magnetic resonance (NMR) spectroscopic, and computational analyses, we show that intramolecular hydrogen bond formation results in two slowly interconverting rotational isomers with a fully planar squaraine backbone.

In one conformer, the amido substituents are located on opposite sides of the molecule (*anti*) and in the other on the same side (*syn*). Titration experiments revealed that the interconversion of the conformers is accelerated in the presence of trifluoroacetic acid.

We started our study by performing an FT-IR spectroscopic analysis to probe the presence of hydrogen bonds in the amide substituted squaraine dye **1**. FT-IR spectra of **1** were recorded in bulk and in chloroform (c = 4 mM) where **1** is molecularly dissolved.[15] Both spectra showed absorption bands at ∼3140 cm^{-1} and ∼3100 cm^{-1} which were attributed to the NH stretching vibration (Figure S1). These bands occur at similar wavenumbers in bulk and in the molecularly dissolved state, indicating that the amide groups of **1** are engaged in the formation of intramolecular hydrogen bonds.[22]

To obtain insights into the nature of the hydrogen bonds, we analyzed the conformation of the squaraine dye computationally. To reduce computational costs, we computed the structure of the homologue **1′** that contains methyl instead of heptyl moieties on the amide groups. We performed a conformational search using the program Macromodel[23] with

Received: April 20, 2021
Published: September 1, 2021

https://doi.org/10.1021/acs.joc.1c00922
J. Org. Chem. 2021, 86, 13100−13103

the OPLS3 force field[24] and a solvent model for chloroform.[25,26] The geometries of the obtained low energy structures were optimized by density functional theory calculations on the B3LYP-D3/6-31G** level.[27−30] The calculations yielded two planar low energy structures (Scheme 2) that suggest complete conjugation of the π-system, which is

Scheme 2. Computational Analysis of *anti*- and *syn*-Conformer As Well As the Transition State of the Isomerization of 1′ in $CHCl_3$

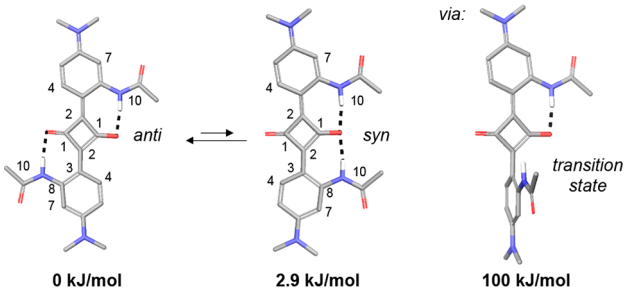

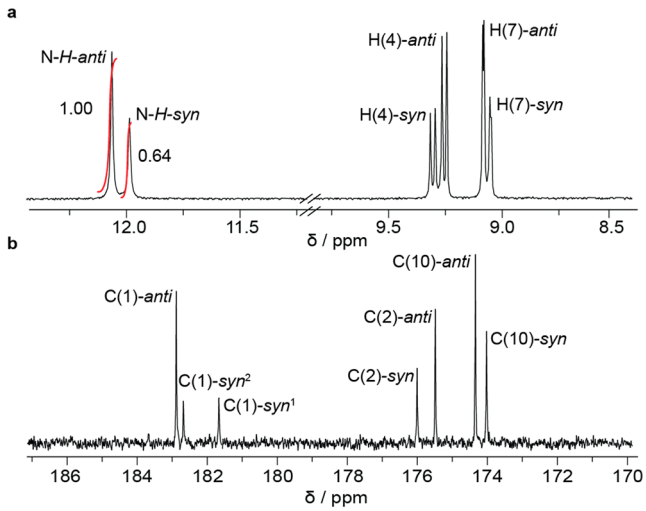

Figure 1. (a) ^{1}H NMR (400 MHz) and (b) ^{13}C{1H} spectrum recorded at room temperature in $CDCl_3$ (100 MHz).

in good agreement with the UV/vis absorption properties of **1**.[15] In both structures, the amide groups form intramolecular hydrogen bonds to the oxo-substituents of the quadratic core. Yet, the structures differ in the relative orientations of the amido substituents. In the lowest energy structure, each amide group is hydrogen bonded to a different oxo-substituent of the quadratic core ("*anti*-conformer"). In contrast, both amido substituents of the second conformer are bonded to the same oxo-substituent ("*syn*-conformer"). The energies of the two conformers differ by only 2.9 kJ/mol, which is similar to the previously reported value for the hydroxy-derivative.[17]

Next, we studied the transition state between the two conformers to determine the activation energy for the rotation about the C(sp^2)−C(sp^2) bond. Using the transition state locator of the program Jaguar, a transition state with a torsion angle of −93° (C(1)−C(2)−C(3)−C(8)) was identified (Scheme 2). This conformer is 100 kJ/mol higher in energy compared to the *anti*-conformer which indicates that both conformers should be observable via e.g. NMR spectroscopy at room temperature.

Encouraged by the computational analysis, we studied **1** in $CDCl_3$ solution by ^{1}H and ^{13}C{1H} NMR spectroscopy (Figure 1; the full spectra with assignment of all signals are depicted in Figure S2 and Table S1). Gratifyingly, both spectra showed the presence of two spin systems in a ratio of 1.00:0.64. The ^{13}C{1H} NMR spectrum was used to assign the two spin systems to the *syn*- and *anti*-conformer. The quadratic core of the major conformer showed one signal for C(1), and that of the minor conformer, two signals. Thus, we attribute the C_{2h} symmetric *anti*-conformer to the major, and the C_{2v} symmetric *syn*-conformer to the minor conformer of **1**. This is in good agreement with the computational analysis that predicted the *anti*-conformer to be more stable than the *syn*-conformer.

The activation energy barriers for the interconversion of the two rotamers were subsequently studied by ^{1}H NMR spectroscopy by following the chemical shifts of the protons in a variable temperature (VT) experiment. The signals that were assigned to N−H, H(4) and H(5) of the two conformers, were fully separated at room temperature and started to partially overlap at 50 °C (Figure S7). Unfortunately, no full coalescence was observed until 61 °C, the boiling point of $CDCl_3$. We reasoned that the rotation about the C(2)−C(3) bond was still hindered at this elevated temperature due to the intramolecular hydrogen bonds. To study the NMR spectrum of **1** at higher temperatures, we replaced $CDCl_3$ by higher boiling 1,1,2,2-tetrachloroethane-d_2 ($C_2D_2Cl_4$). Interestingly, the preference for the *anti*-conformer observed in $CDCl_3$ changed to a preference for the *syn*-conformer in $C_2D_2Cl_4$ with a change in *anti*/*syn* ratio from 1.00:0.64 ($CDCl_3$) to 0.70:1.00 ($C_2D_2Cl_4$). We attribute this reversal of conformer stability to small enthalpic and entropic changes in the solvation.[31] The coalescence of the two spin systems in $C_2D_2Cl_4$ was reached at 64 °C (Figure S8).

A common approximation for the analysis of the line broadening to determine the free energy of activation of rotamers is given by Eyring's equations as modified by Shanan-Atidi (for details see Supporting Information).[32−35] The calculation yielded an activation energy barrier $\Delta G^{\ddagger}_{anti}$ (between *anti*-conformer and the transition state) of 73 ± 1 kJ/mol and $\Delta G^{\ddagger}_{syn}$ 75 ± 1 kJ/mol (between *syn*-conformer and the transition state).

If the comparatively high activation energy is due to the formation of the intramolecular hydrogen bonds, we reasoned, that addition of a hydrogen-bond breaking additive such as trifluoroacetic acid (TFA) would lower the barrier between the two conformers. The ^{1}H NMR spectra of **1** in $CDCl_3$ indeed change upon addition of 0.01, 0.05, 0.07, and 0.10 vol % TFA-d_1 (Figure 2; full spectra in Figure S9). The spectrum of **1** in the presence of 0.01 vol % TFA-d_1 exhibited spectral broadening of the signals suggesting a reduced coalescence temperature. This effect was more pronounced for higher amounts of TFA-d_1 (0.03 vol %, 0.05 vol %). Full coalescence was observed when 0.10 vol % TFA-d_1 was added, which suggested a coalescence temperature of equal or below room temperature.

The same trend is also reflected in the corresponding activation energies: $\Delta G^{\ddagger}_{syn}/\Delta G^{\ddagger}_{anti}$ decreases from >70/>72 kJ/mol (0.01 vol % TFA-d_1, T_c > 50 °C; Figure S10), to 69 ± 1/72 ± 1 kJ/mol (0.05 vol % TFA-d_1, T_c = 45 °C; Figure S11) and 67 ± 1/69 ± 1 kJ/mol (0.07 vol % TFA-d_1, T_c = 35 °C; Figure S12). The lowest activation energies were observed for

https://doi.org/10.1021/acs.joc.1c00922
J. Org. Chem. 2021, 86, 13100−13103

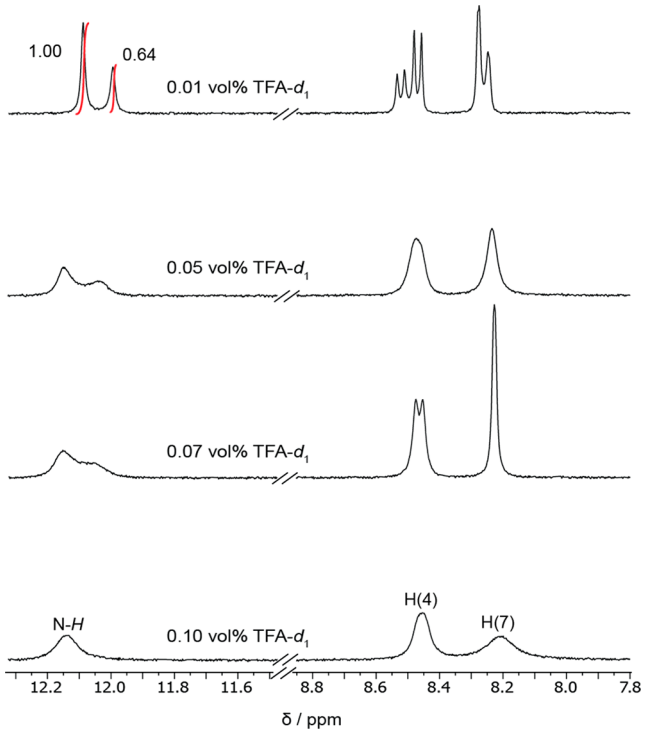

Figure 2. ^{1}H NMR spectrum (400 MHz) of **1** in $CDCl_3$ (c = 6.6 mM) at room temperature upon addition of 0.01−0.10 vol % TFA-d_1.

at 0.10 vol % TFA-d_1 with <64/<67 kJ/mol (0.10 vol % TFA-d_1, T_c < 25 °C).

In conclusion, conformational analysis of the amide substituted squaraine dye **1** showed the presence of a *syn*- and *anti*-conformer stabilized by intramolecular hydrogen bonds. The two conformers differ in the orientation of the amido substituents that are located either on opposite sides of the molecule (*anti*) or on the same side (*syn*). Already small amounts of TFA-d_1 disrupt the intramolecular hydrogen bonds and accelerate the conformer interconversion. Hence, minute quantities of TFA can prevent the formation of e.g. kinetically trapped conformers that might lead to pathway complexity resulting in unexpected or irreproducible properties of supramolecular systems.

EXPERIMENTAL SECTION

Materials and Methods. The synthesis of **1** was performed according to literature procedure.[15]

^{1}H, ^{13}C{^{1}H} and 2D NMR Spectra. A Varian Mercury Vx 400 MHz was utilized to record ^{1}H, ^{13}C{^{1}H} and 2D NMR spectra. Deuterated solvents were purchased from Cambridge Isotope Laboratories and are indicated for each measurement. Chemical shifts (δ) are expressed in ppm, and are referred to the residual peak of the solvent.

FT-IR Spectra. A PerkinElmer Spectrum One spectrometer was used to record FT-IR spectra. The investigated solutions were prepared by weighing the required amount of compound and transferring it into a screw-capped vial. The desired concentration (4 mM) was adjusted by the addition of the chosen solvent by using Gilson MICROMAN Positive-Displacement Pipets. The samples were heated and sonicated until homogeneous solutions were obtained. The measurements were performed in a fluorine doped tin oxide coated glass slide cuvette (100 mm × 100 mm × 2.3 mm, surface resistivity 7 W/sq, 32 scans).

Computational Analyses. Computational analyses were performed on a derivative of **1** with two acetamide substituents **1′** to reduce computational cost. Conformational searches (5.000 steps) were performed using MacroModel 11.0 with the OPLS3 force field in $CDCl_3$ and a cutoff of 21 kJ/mol. The search provided two conformers (*syn* and *anti*). The geometry was optimized using Jaguar at the B3-LYP-D3/6-31G** level of theory. Both structures show no imaginary frequency (Total free energies (vacuum): *syn*-conformer = −1450.240173 au, *anti*-conformer = −1450.241602 au). Optimization with solvation corrections was performed on gas-phase geometries using a PBF implicit solvent model for $CHCl_3$. The population of the structures was calculated according to the Boltzmann distribution. The transitions state was located using the transition state search module of Jaguar using both conformers (*syn* and *anti*) as reference points for a search along the lowest Hessian eigenvector at the B3-LYP-D3/6-31G** level of theory. One imaginary frequency was observed (Total free energy (vacuum): −1450.201998 au; imaginary frequency: −13.8 cm^{-1}). Optimization with solvation corrections was performed on gas-phase geometries using a PBF implicit solvent model for $CHCl_3$.

ASSOCIATED CONTENT

Supporting Information

The Supporting Information is available free of charge at https://pubs.acs.org/doi/10.1021/acs.joc.1c00922.

Spectroscopic and computational data as well as calculation of the activation energy barriers (PDF)

AUTHOR INFORMATION

Corresponding Author

Tobias Schnitzer − *Laboratory of Macromolecular and Organic Chemistry, and Institute for Complex Molecular Systems, Department of Chemical Engineering and Chemistry, Eindhoven University of Technology, 5600 MB Eindhoven, The Netherlands;* orcid.org/0000-0003-3613-576X; Email: t.schnitzer@tue.nl

Authors

Andreas T. Rösch − *Laboratory of Macromolecular and Organic Chemistry, and Institute for Complex Molecular Systems, Department of Chemical Engineering and Chemistry, Eindhoven University of Technology, 5600 MB Eindhoven, The Netherlands*

Serge H. M. Söntjens − *Laboratory of Macromolecular and Organic Chemistry, and Institute for Complex Molecular Systems, Department of Chemical Engineering and Chemistry, Eindhoven University of Technology, 5600 MB Eindhoven, The Netherlands;* orcid.org/0000-0001-5939-6925

Jorn Robben − *Laboratory of Macromolecular and Organic Chemistry, and Institute for Complex Molecular Systems, Department of Chemical Engineering and Chemistry, Eindhoven University of Technology, 5600 MB Eindhoven, The Netherlands*

Anja R. A. Palmans − *Laboratory of Macromolecular and Organic Chemistry, and Institute for Complex Molecular Systems, Department of Chemical Engineering and Chemistry, Eindhoven University of Technology, 5600 MB Eindhoven, The Netherlands;* orcid.org/0000-0002-7201-1548

Complete contact information is available at: https://pubs.acs.org/10.1021/acs.joc.1c00922

Funding

The authors acknowledge funding from the Dutch Ministry of Education, Culture and Science (Gravity program 24.001.035).

T.S. thanks the Swiss National Science Foundation for a Postdoc.Mobility fellowship.

Notes

The authors declare no competing financial interest.

■ ACKNOWLEDGMENTS

We thank Prof. E. W. Meijer for fruitful discussions.

■ REFERENCES

(1) Grande, V.; Shen, C.-A. A.; Deiana, M.; Dudek, M.; Olesiak-Banska, J.; Matczyszyn, K.; Würthner, F. Selective Parallel G-Quadruplex Recognition by a NIR-to-NIR Two-Photon Squaraine. *Chem. Sci.* **2018**, *9*, 8375−8381.

(2) Shaw, S. K.; Liu, W.; Gómez Durán, C. F. A.; Schreiber, C. L.; de Betancourt Mendiola, M. L.; Zhai, C.; Roland, F. M.; Padanilam, S. J.; Smith, B. D. Non-Covalently Pre-Assembled High-Performance Near-Infrared Fluorescent Molecular Probes for Cancer Imaging. *Chem. - Eur. J.* **2018**, *24*, 13821−13829.

(3) Philips, D. S.; Ghosh, S.; Sudheesh, K. V.; Suresh, C. H.; Ajayaghosh, A. An Unsymmetrical Squaraine-Dye-Based Chemical Platform for Multiple Analyte Recognition. *Chem. - Eur. J.* **2017**, *23*, 17973−17980.

(4) Babu, P. S. S.; Manu, P. M.; Dhanya, T. J.; Tapas, P.; Meera, R. N. Photodynamic Therapy Disrupts Redox Homeostasis and Induce Mitochondria-Mediated Apoptosis in Human Breast Cancer Cells. *Sci. Rep.* **2017**, *7*, 42126.

(5) Schulz, M.; Mack, M.; Kolloge, O.; Lützen, A.; Schiek, M. Organic Photodiodes from Homochiral L-Proline Derived Squaraine Compounds with Strong Circular Dichroism. *Phys. Chem. Chem. Phys.* **2017**, *19*, 6996−7008.

(6) Schulz, M.; Balzer, F.; Scheunemann, D.; Arteaga, O.; Lützen, A.; Meskers, S. C. J.; Schiek, M. Chiral Excitonic Organic Photodiodes for Direct Detection of Circular Polarized Light. *Adv. Funct. Mater.* **2019**, *29*, 1900684.

(7) Cheon, J. H.; Kim, S. A.; Ahn, K. S.; Kang, M. S.; Kim, J. H. Enhanced Light-Harvesting Efficiency by Förster Resonance Energy Transfer in Quasi-Solid State DSSC Using Organic Blue Dye. *Electrochim. Acta* **2012**, *68*, 240−245.

(8) Matsui, M.; Haishima, Y.; Kubota, Y.; Funabiki, K.; Jin, J.; Kim, T. H.; Manseki, K. Application of Benz[c, d]Indolenine-Based Unsymmetrical Squaraine Dyes to near-Infrared Dye-Sensitized Solar Cells. *Dyes Pigm.* **2017**, *141*, 457−462.

(9) Gräf, K.; Rahim, M. A.; Das, S.; Thelakkat, M. Complementary Co-Sensitization of an Aggregating Squaraine Dye in Solid-State Dye-Sensitized Solar Cells. *Dyes Pigm.* **2013**, *99*, 1101−1106.

(10) Klein, M.; Pankiewicz, R.; Zalas, M.; Stampor, W. Magnetic Field Effects in Dye-Sensitized Solar Cells Controlled by Different Cell Architecture. *Sci. Rep.* **2016**, *6*, 30077.

(11) Varma, P. C. R.; Namboothiry, M. A. G. Squaraine Based Solution Processed Inverted Bulk Heterojunction Solar Cells Processed in Air. *Phys. Chem. Chem. Phys.* **2016**, *18*, 3438−3443.

(12) Brück, S.; Krause, C.; Turrisi, R.; Beverina, L.; Wilken, S.; Saak, W.; Lützen, A.; Borchert, H.; Schiek, M.; Parisi, J. Structure-Property Relationship of Anilino-Squaraines in Organic Solar Cells. *Phys. Chem. Chem. Phys.* **2014**, *16*, 1067−1077.

(13) Law, K. Y. Organic Photoconductive Materials: Recent Trends and Developments. *Chem. Rev.* **1993**, *93*, 449−486.

(14) Sreejith, S.; Carol, P.; Chithra, P.; Ajayaghosh, A. Squaraine Dyes: A Mine of Molecular Materials. *J. Mater. Chem.* **2008**, *18*, 264−274.

(15) Rösch, A. T.; Zhu, Q.; Robben, J.; Tassinari, F.; Meskers, S.; Naaman, R.; Palmans, A.; Meijer, E. W. Helicity Control in the Aggregation of Achiral Squaraine Dyes in Solution and Thin Films. *Chem. - Eur. J.* **2021**, *27*, 298−306.

(16) Yang, L.; Zhu, Y.; Jiao, Y.; Yang, D.; Chen, Y.; Wu, J.; Lu, Z.; Zhao, S.; Pu, X.; Huang, Y. The Influence of Intramolecular Noncovalent Interactions in Unsymmetrical Squaraines on Material Properties, Film Morphology and Photovoltaic Performance. *Dyes Pigm.* **2017**, *145*, 222−232.

(17) Kazmaier, P. M.; Hamer, G. K.; Burt, R. A. Conformational Isomerism in Squaraines: Saturation Transfer NMR Studies on Hydroxy Squaraines. *Can. J. Chem.* **1990**, *68*, 530−536.

(18) Liu, T.; Liu, X.; Wang, W.; Luo, Z.; Liu, M.; Zou, S.; Sissa, C.; Painelli, A.; Zhang, Y.; Vengris, M.; Bondar, M. V.; Hagan, D. J.; Van Stryland, E. W.; Fang, Y.; Belfield, K. D. Systematic Molecular Engineering of a Series of Aniline-Based Squaraine Dyes and Their Structure-Related Properties. *J. Phys. Chem. C* **2018**, *122*, 3994−4008.

(19) Diehl, K. L.; Bachman, J. L.; Anslyn, E. V. Tuning Thiol Addition to Squaraines by Ortho-Substitution and the Use of Serum Albumin. *Dyes Pigm.* **2017**, *141*, 316−324.

(20) Cox, J. R.; Müller, P.; Swager, T. M. Interrupted Energy Transfer: Highly Selective Detection of Cyclic Ketones in the Vapor Phase. *J. Am. Chem. Soc.* **2011**, *133*, 12910−12913.

(21) Bacher, E. P.; Koh, K. J.; Lepore, A. J.; Oliver, A. G.; Wiest, O.; Ashfeld, B. L. A Phosphine-Mediated Dearomative Skeletal Rearrangement of Dianiline Squaraine Dyes. *Org. Lett.* **2021**, *23*, 2853−2857.

(22) Timme, A.; Kress, R.; Albuquerque, R. Q.; Schmidt, H. W. Phase Behavior and Mesophase Structures of 1,3,5-Benzene- and 1,3,5-Cyclohexanetricarboxamides: Towards an Understanding of the Losing Order at the Transition into the Isotropic Phase. *Chem. - Eur. J.* **2012**, *18*, 8329−8339.

(23) *MarcoModel*, Version 11.4; Schrödinger, LLC, Schrödinger Release 2017-4: New York, NY, 2017.

(24) Harder, E.; Damm, W.; Maple, J.; Wu, C.; Reboul, M.; Xiang, J. Y.; Wang, L.; Lupyan, D.; Dahlgren, M. K.; Knight, J. L.; Kaus, J. W.; Cerutti, D. S.; Krilov, G.; Jorgensen, W. L.; Abel, R.; Friesner, R. A. OPLS3: A Force Field Providing Broad Coverage of Drug-like Small Molecules and Proteins. *J. Chem. Theory Comput.* **2016**, *12*, 281−296.

(25) Still, W. C.; Tempczyk, A.; Hawley, R. C.; Hendrickson, T. Semianalytical Treatment of Solvation for Molecular Me-Chanics and Dynamics. *J. Am. Chem. Soc.* **1990**, *112*, 6127−6129.

(26) Qiu, D.; Shenkin, P. S.; Hollinger, F. P.; Still, W. C. The GB/SA Continuum Model for Solvation. A Fast Analytical Methodfor the Calculation of Approximate Born Radii. *J. Phys. Chem. A* **1997**, *101*, 3005−3014.

(27) Bochevarov, A. D.; Harder, E.; Hughes, T. F.; Greenwood, J. R.; Braden, D. A.; Philipp, D. M.; Rinaldo, D.; Halls, M. D.; Zhang, J.; Friesner, R. A. Jaguar: A High-Performance Quantum Chemistry Software Program with Strengths in Life and Materials Sciences. *Int. J. Quantum Chem.* **2013**, *113*, 2110−2142.

(28) Lee, C.; Yang, W.; Parr, R. G. Development of the Colle-Salvetti Correlation-Energy Formula into a Functional of the Electron Density. *Phys. Rev. B: Condens. Matter Mater. Phys.* **1988**, *37*, 785.

(29) Miehlich, B.; Savin, A.; Stoll, H.; Preuss, H. Results Obtained with the Correlation Energy Density Functionals of Becke and Lee, Yang and Parr. *Chem. Phys. Lett.* **1989**, *157*, 200−206.

(30) Krishnan, R.; Binkley, J. S.; Seeger, R.; Pople, J. A. Self-Consistent Molecular Orbital Methods. XX. A Basis Set for Correlated Wave Functions. *J. Chem. Phys.* **1980**, *72*, 650−654.

(31) For examples, see: (a) Konopacka, A.; Pawelka, Z. Aromatic Solvent Effect on the Rotational Isomerism in 2-Hydroxy-5-Methyl-3-Nitroacetophenone. *J. Phys. Org. Chem.* **2005**, *18*, 1190−1195. (b) Schnitzer, T.; Wennemers, H. Influence of the *Trans*/*Cis* Conformer Ratio on the Stereoselectivity of Peptidic Catalysts. *J. Am. Chem. Soc.* **2017**, *139*, 15356−15362.

(32) Bovey, F. A. *Nuclear Magnetic Resonance Spectroscopy*; Academic Press: New York, 1969.

(33) Pople, H. A.; Schneider, W. G.; Bernstein, H. J. *High Resolution Nuclear Magnetic Resonance*; McGraw-Hill: New York, 1967.

(34) Shanan-Atidi, H.; Bar-Eli, K. H. A Convenient Method for Obtaining Free Energies of Activation by the Coalescence Temperature of an Unequal Doublet. *J. Phys. Chem.* **1970**, *74*, 961−963.

(35) Frank, J. H.; Powder-George, Y. L.; Ramsewak, R. S.; Reynolds, W. F. Variable-Temperature 1H-NMR Studies on Two C-Glycosylflavones. *Molecules* **2012**, *17*, 7914−7926.

https://doi.org/10.1021/acs.joc.1c00922
J. Org. Chem. 2021, 86, 13100−13103